Available online at www.sciencedirect.com

ScienceDirect

Procedia Manufacturing 41 (2019) 304–311

Procedia MANUFACTURING

www.elsevier.com/locate/procedia

8th Manufacturing Engineering Society International Conference

Determination of emissivity and temperature of tool rake face when cutting AISI 4140

D. Soler[a]*, P. X. Aristimuño[a], M. Saez-de-Buruaga[a], P. J. Arrazola[a]

[a]*Mechanics and industrial production department, Faculty of Engineering-Mondragon Unibertsitatea, Mondragon, Spain*

Abstract

A method for measuring tool temperature in the tool/chip contact zone of the rake face of a tool during dry orthogonal cutting using thermography is presented. This method used a new calibration method that combined with a standard camera calibration allows to estimate surface emissivity. The effect of material deposition and tool oxidation on the emissivity is analyzed. These techniques effectively showed thermal field on the rake face when machining AISI 4140.

Keywords: Emissivity; Infrared Thermography; Metal Cutting

1. Introduction

The experimental investigation of heat generation occurring in metal cutting has received much attention in the last decades [1]. The temperature reached in the tool is an indirect measurement of heat produced due to the high plastic deformation of the material, and tool-chip and tool-workpiece friction [2]. It is well established that tool-chip interface temperatures have very significant influence on final workpiece quality [3] and on tool wear [4].

There are many available techniques to measure temperatures such as thermocouples [5], thermistor [6], resistance temperature detector [7], these techniques are intrusive and are difficult to use in order to obtain thermal gradients. Infrared thermography is an advanced measurement technology that transforms surface infrared electromagnetic radiation into a digital signal [8–10]. The main advantages of this technology are: i) it is non-intrusive; ii) it allows

* Corresponding author. Tel.: +34 943-794-700;
E-mail address: dsoler@mondragon.edu

full field measurements; iii) it has high-speed response. However, it has also some drawbacks: i) equipment cost; ii) difficulty to measure temperatures when lubricants are used; iii) define an appropriate methodology to obtain accurate measurements.

Empirical models for predicting cutting behavior in machining could be classified in two groups: mechanistic models, based on experimental results obtained from cutting operation (turning, drilling, boring process and so on) [11,12]; and orthogonal models, based on experimental data obtained from fundamental orthogonal cutting tests. Orthogonal models development requires simpler and cheaper set-ups, and are able to obtain material database with which predict cutting performance for any machining operation, [13,14]. For this reason in the present study only orthogonal cutting was considered. The difficulty to measure temperature using infrared technologies when lubricants are used yields to limit our self to dry orthogonal tests.

To measure tool temperature fields in the tool/chip contact zone using infrared technology two techniques can be found in the literature: i) the use of transparent tools [15,16], and ii) the introduction of artificial slots on the workpiece, allowing a clear view of the tool/chip contact zone, without the chip obstruction [17,18]. However, taking into account that the temperature strongly depends on contact material pair, that is, of the friction coefficient between the tool and the chip, and transparent tools are not commonly used in the industry, the authors decided to use the second technique in the present study.

This technique roughly consists in performing a small slot in the workpiece to be machined with the aim to be able to observe the tool/chip contact zone, when the tool reaches the slot. In this particular case, the workpieces were tubes in which some predefined slots were cut. These tubes were placed in a vertical CNC machining center. The infrared camera was placed in front of the rake face of the tool.

During the filming, there were two different situations: the first situation when the tool was cutting the workpiece (Fig. 1 a)). And the second situation, when the tool reaches a slot (Fig. 1 b)). In the first situation the chips flow prevent tool/chip contact zone to be observed with the camera. However, it was possible to measure temperatures in the overhang, at the right of the contact zone, and in the inner zone of the tool, at the left of the contact zone. In the second situation, the chip was removed and a clear vision of the rake face could be obtained, making it possible to determine temperature distribution in the rake face.

a) b)

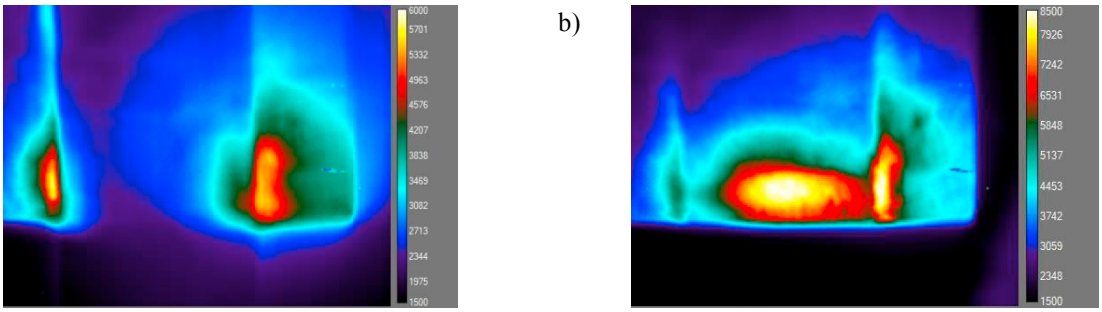

Fig 1. a) Thermography of tool's rake face when cutting the workpiece; b) Thermography of the tool/chip contact zone (2nd situation).

When thermography is used, the calibration technique of the infrared thermometer and the radiation surface emissivity estimation is crucial in order to obtain realistic temperature values from camera digital signal output [19]. The novel calibration method showed in our previous study [20] allows to obtain temperature fields without the need for emissivity correction. However, combining this calibration method with a standard camera calibration it is possible to estimate the emissivity of radiating surface. Moreover, during the cutting two important phenomena occurs that deals with temperature measurements using Infrared techniques because might locally change the emissivity of a surface: i) surface oxidation [21] and ii) material deposition [22].

The main goal of the present work is to use these two calibration methods to make a quantitative estimation of the influence of oxidation and material deposition in the emissivity of the tool's rake face.

2. Methodology

The experimental procedure is explained in a previous publication [17]. In this case, workpiece are tubes of AISI 4140 steel. Tubes had 50 ± 0.05 mm external diameter and a wall thickness of 1 ± 0.02 mm. The samples were mounted on a vertical Lagun HS 1000 vertical CNC machining center which controlled the cutting conditions; cutting velocity (v_c = 250 m/min) and feed rate (f = 0.2 mm/rev). The uncoated P10 carbide tool, with plane rake face and an edge radius of 5 µm (SPUN 120308 P10) was attached to a tool holder, which was placed over a 3-component dynamometer (Kisler 9121) allowing to measure cutting and feed forces during the cut. The infrared camera was a FLIR Titanium 550M, equipped with a macroscopic lens giving a spatial resolution of 1 pixel=10 µm and a narrow-band filter in the IR spectral range of 3.97–4.01 µm, IR image resolution was of 208×162 pixels, and the frame rate of 832.1 Hz.

Three tests were carried out at the same cutting conditions. For each test, a new tool was used in order to prevent undesirable effects of the tool wear. In the present study, two calibrations methods are used: the new calibration method published in [20] and a standard camera calibration [23].

The standard calibration is a curve relating recorded radiation (expressed in Digital Levels – DL) when the infrared camera is placed in front a blackbody cavity and the blackbody temperature. This curve is usually supplied by the camera manufacturer. Therefore, when a standard calibration is used to interpret an IR image, the obtained temperature field does not correspond to the real temperature of the emitting target surface, but to the temperature of a blackbody emitting the same radiation as this surface, usually called Radiation Temperature (RT). In order to know the real temperature it is necessary to know the spectral emissivity (ε(λ,T)) of the emitting surface that relates the spectral radiance of the real object with that of the blackbody. In general, it is assumed that emitting surface corresponds to a graybody, i.e., the spectral emissivity is constant for all wavelength. In the present case, this is not a strong assumption because of the narrow-band filter used.

According to this, combining both calibration methods, it is possible to estimate the emissivity of the tool rake face using equation (1).

$$\frac{1}{T} = \frac{1}{RT} + \frac{\lambda}{C_\omega}\log(\varepsilon) \tag{1}$$

where C_ω = 14.389·10^3 Kµm is the second radiation constant, and ε is the emissivity of the target surface at the λ wavelength.

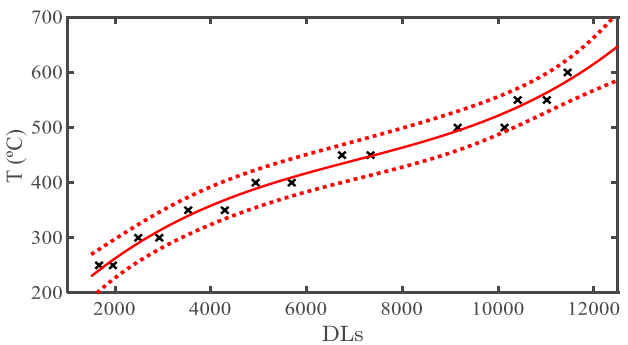

Fig 2. Calibration curve of SPUN100308 P10 tool with integration time of 200 µs. Experimental data and fitted polynomial.

The new calibration method allows to directly relate DLs with the real temperature (T) without the need of the emissivity. Basically, this method consists of heating the tool with an induction system and record emitted radiation in the same conditions as those used during the cutting process. Tool temperature is controlled with thermocouples, therefore, being possible to fit an interpolating function, which corresponds to the calibration curve, see Fig 2 This

calibration was made placing the insert inside a hermetic box with a controlled atmosphere of Argon, in order to prevent metal oxidation.

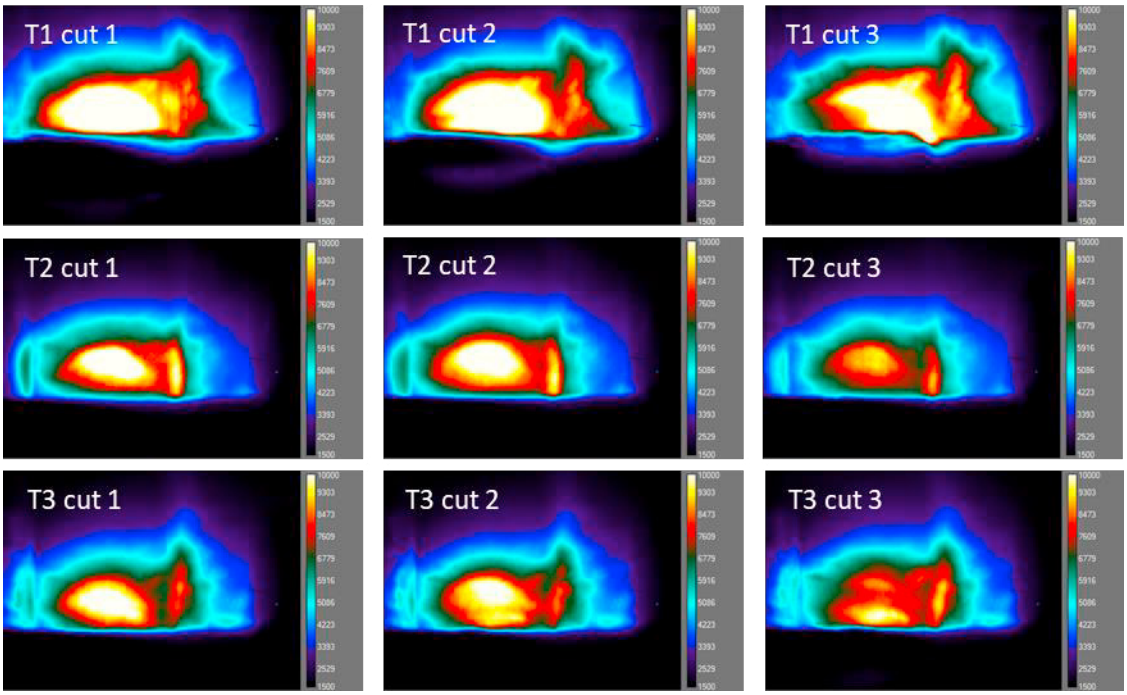

Fig 3 IR images of the rake face when machining AISI414.

3. Results

As stated in the introduction, when the tool reached the workpiece slot it was possible to observe the rake face of the tool. However, in order to have a clear view of the rake face, no chip could be retained between the tool and the camera. Unfortunately in all performed tests, the first time the tool reached the slot, chip obstructed a clear view of the rake face; however, in posterior interrupted cuttings this drawback did not occur. Fig 3 shows nine different thermographies (three cuts for each test) of the rake face of the tool, obtained using FLIR ResearchIR Max®.

Table 1. Values of maximum temperature in the rake face obtained from IR image, and distance to the cutting edge.

Test	Maximum temperature (ºC)	Distance to the cutting edge (mm)
Test 1 cut 1	686	0.15
Test 1 cut 2	712	0.13
Test 1 cut 3	624	0.15
Test 2 cut 1	586	0.28
Test 2 cut 2	569	0.35
Test 2 cut 3	510	0.24
Test 3 cut 1	561	0.23
Test 3 cut 2	543	0.32
Test 3 cut 3	527	0.10

Used Infrared camera sensors had a linear response to the incident radiance. Therefore, while DL values had no physical meaning, observing these images it is possible to extract some conclusions: i) radiation observed during the first test was higher than in the others. In this test it is also possible to observe that the cutting edge had suffered a higher wear. ii) In the third test, maximum radiation point seems to be nearer the cutting edge than in the other cases. The values collected in Table 1 confirm above exposed observation.

With the help of Matlab, it is possible to apply to each image the interpolating function plotted in Fig 2 and then obtain temperature fields. For all tests, the maximum temperature recorded in the chip/tool contact zone was computed, and the obtained values are available in Table 1. This maximum value is placed at a certain distance of the cutting edge, which is shown in the third row of Table 1.

As it can be seen in Table 1, temperatures achieved during the test 1 were significantly higher. The mean temperature during tests 2 and 3 was 549 ± 28 ºC, while in the first test mean temperature was 674 ± 45 ºC, which suppose an increase of 23%. The tool wear observed could explain the temperature increase. The different position where the maximum temperature were observed could confirm this supposition, indeed, it reveals a change in the cut dynamics. Forces were measured during the tests and no significant differences were observed between tests (less than 1.3% in the cutting force and 3.2% in feed force). This suggests that temperature measurements could be better indicators of tool wear than force measurements.

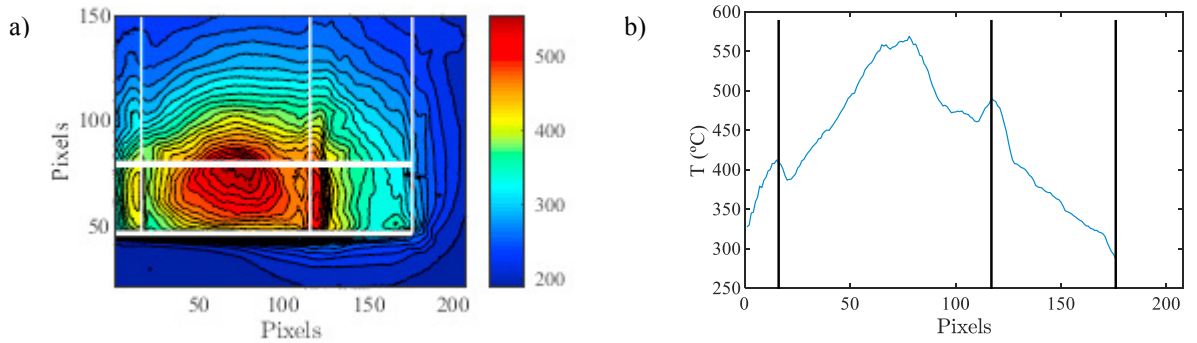

Fig 4 a) Temperature field of the rake face of 2nd cut of Test 2. b) Temperature on the straight line parallel to the cutting edge highlighted in a).

Fig 4 a) shows the temperature field corresponding to Test 2 cut 2, and Fig 4 b) shows the temperature on the straight line parallel to the cutting edge placed over the point where the maximum temperature is observed. A very strange phenomenon is observed in Fig 4 b), where two local maxima could be seen just in the vicinity of the tool/chip contact zone. Similar temperature profiles were observed in all tests.

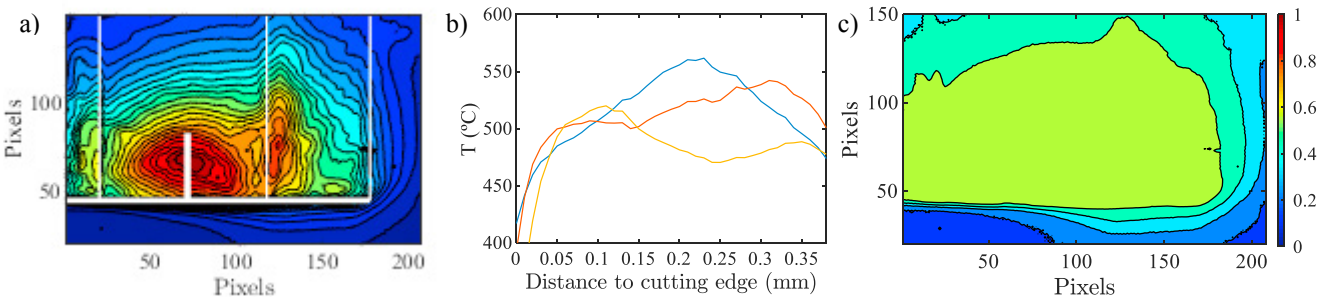

Fig 5 a) Temperature field of the rake face. b) Temperature over the line highlighted in test 2. c) Estimated emissivity of the tool.

Regarding test 2 and 3, the maximum temperature is placed at roughly 0.28 mm of the cutting edge. However, in the case of test 3 cut 3 this maximum is placed much nearer to the cutting edge. Fig 5 is useful to better observe this phenomenon. Fig 5 a) shows temperature field in the rake face of test 3 cut 1, where a line orthogonal to the cutting edge is highlighted. Fig 5 b) shows temperature over that line in the three consecutive cuts. A local maximum can be appreciated, which appears at a distance of about 0.07 mm of the cutting edge.

Finally, as can be observed in Fig 5 c), using temperature fields obtained with both calibrations and with the help of equation (1), it is possible to estimate that the emissivity of the tool is 0.60 ± 0.01 when the temperature is about 510 ± 50 ºC.

4. Discussion

4.1. Local maxima in the neighborhood of the tool/chip cutting zone: oxidation

It is clear that the heat source during the cutting is placed in the tool/chip contact zone. Therefore, maximum temperature in the tool rake face is achieved in this zone. Consequently, the two local maximum placed near the tool/chip contact zone showed in Fig 4 b) does not correspond to a physical reality. When the calibration curve was used to compute temperature values from camera DL, it was used for all pixel/detectors, assuming implicitly that the emissivity had the same value for whole tool (see Fig 5 c)). However, it might be local emissivity changes. Due to heat conduction, during the cut, the overhang and inner tool also achieved high temperatures, both zones were in contact with the air, and therefore, they were susceptible to oxidation. When a thin layer of oxides attached the surface of a metal, the corresponding emissivity of this surface changes. An increase of emissivity will imply an increase of emitted radiation. This could explain the local maximum of Fig 4 b).

In order to check above exposed hypothesis, used tool were inspected in a Scanning Electron Microscope (SEM) with Energy dispersive X-ray spectrometer. As showed in our previous work [20], an important presence of oxygen in the overhang next to the tool/chip contact zone was observed, while no relevant presence of oxygen were observed in the tool/chip contact zone.

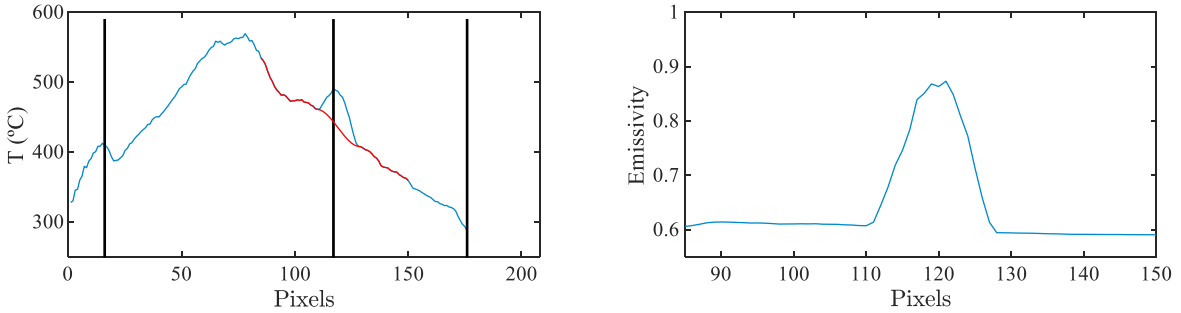

Fig 6 a) Real temperature in the vicinity of the tool/chip contact zone; b) emissivity of each pixel of the vicinity.

Assuming continuity and monotonicity of temperatures between pixels 85 and 150 in Fig 6 a), it was possible to estimate the real temperature in the tool/chip contact zone vicinity. These corrected values, and radiation temperatures obtained from the standard calibration were introduced into equation (1) to compute the local emissivity this zone.

As can be observed in Fig 6 b), tool oxidation yields a significant increase of the emissivity, about 45%, being the same value that was obtained for the local maximum placed in the inner zone. When this calculus was performed along another straight line parallel to the cutting edge, but placed where the maximum in the overhang was found, the emissivity increase up to 47%. Moreover, when other cuts are considered, local emissivity growth of up to 57% was observed.

When tools were inspected in the SEM, no relevant presence of oxygen was found far from the tool/chip contact zone, where the temperature was lower. This fact shows that the oxidation mechanism activates at a certain temperature, according to the authors observation those tools begins oxidizing around 350 ºC. Therefore, a deep study of oxide layer could give a roughly information of the range of temperatures achieved during the cut.

On the other hand, one of the main problems during the cutting is to evacuate heat from the cutting zone. There are three main mechanisms: heat is evacuated from the cutting zone, by removing the hot chip from this zone; heat conduction throughout the tool into the tool holder and far away; and finally, heat radiation. The fact that in the present case the tool emissivity increased with the oxidation suggest that it could be convenient to use oxidized tools, especially, in areas not used for cutting.

4.2. Local maxima appearing near the cutting edge: deposition

Focusing in the test 3, Fig 7 shows the temperature fields of the rake face and the corresponding profiles of vertical lines orthogonal to the cutting edge. For each cut, three lines are plotted, one passing throughout the point where the maximum temperature was detected and one more at each side. The three cuts were consecutive. In profile figures, it is easy to see how a local maximum appears near the cutting edge, being, at the third cut, more relevant that maximum placed at 0.28 mm of the cutting edge.

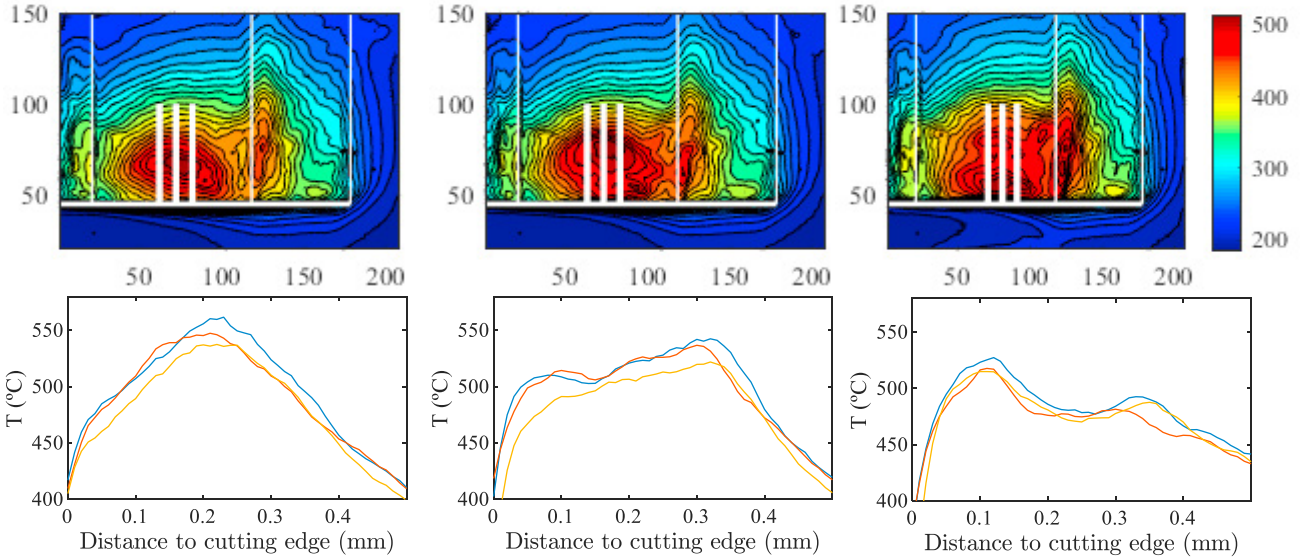

Fig 7 Temperature fields and temperature profiles of vertical highlighted lines during test 3.

This growing maximum was caused by material deposit ion in tool rake face, this material deposition was confirmed in the SEM [20]. Material deposition obviously alters the radiating surface finishing, therefore corresponding emissivity. However, tool geometry could also locally be changed, hence, the dynamics of the cut might also be changed.

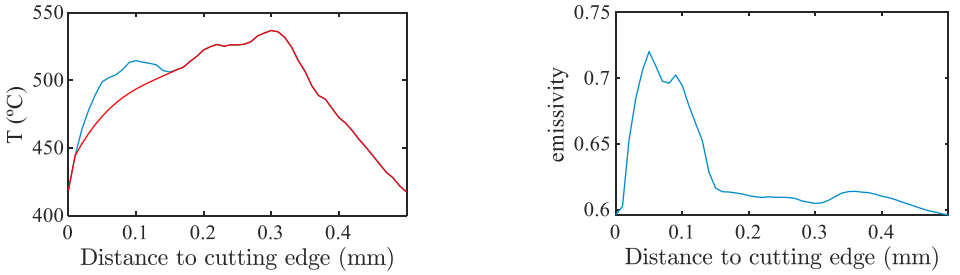

Fig 8 a) Real temperature profile the vertical line of test 2 cut 2. b) Emissivity along the vertical line.

Considering the temperature profile of the first and second cuts, it seems reasonable to state that when the first cut was filmed there was no deposition in the rake face, while in the second cut it was.

Taking into account that the maximum placed far of the cutting edge has very similar values in these two cuts, it can be supposed that between these two instants the cut dynamics had not suffered essential changes. Therefore, the new local maximum could be explained by a local emissivity change. Following the procedure exposed in the previous section, this emissivity change can be estimated (see Fig 8). In this case, the emissivity increase due to material deposition is about 13%.

5. Conclusions and further work

An set-up using infrared technology to measure the temperature in the tool/chip contact zone has been described and used when machining AISI 4140. Assuming the temperature monotonicity of the temperature in the vicinity of the tool/chip contact zone, a procedure to estimate the emissivity of the tool has been used to show that:

- Emissivity significantly changes when the tool oxidizes. Changes up to 55% were reported.
- The tool oxidation mechanism activates at certain temperature. For the uncoated P10 carbide tool around 350 ºC.
- Emissivity significantly changes when material deposition occurs. Changes about 13% were reported.

This study suggests that in order to estimate tool wear, temperature could be a better indicator than forces, being this an interesting field to be explored.

Finally, a deep study of oxidation mechanism and its dynamics it is necessary to evaluate the convenience of use of oxidized tool for an improvement of heat evacuation.

Acknowledgements

This work was supported by the Basque Government within the project MECAERO (PIBA 2018-85) and the Spanish Government within the project EMULATE (DP12015-67667-C3-3R).

References

[1] Davies MA, Ueda T, M'saoubi R, Mullany B, Cooke AL. On the measurement of temperature in material removal processes. CIRPAnnalsManufacturingTechnology (2007);56:581–604.
[2] Childs T, Maekawa K, Obikawa T, Yamane Y. Metal machining: theory and applications. Butterworth-Heinemann; (2000).
[3] Jawahir I, Brinksmeier E, M'Saoubi R, Aspinwall D, Outeiro J, Meyer D, et al. Surface integrity in material removal processes: Recent advances. CIRPAnnalsManufacturingTechnology (2011);60:603–626.
[4] Takeyama H, Murata R. Basic investigation of tool wear. Journal engineeringIndustry (1963);85:33–37.
[5] Martínez DS, Illán F, Solano JP, Viedma A. Embedded thermocouple wall temperature measurement technique for scraped surface heat exchangers. AppliedThermalEngineering (2017);114:793–801.
[6] Stankovic SB, Kyriacou PA. The effects of thermistor linearization techniques on the T-history characterization of phase change materials. AppliedThermalEngineering (2012);44:78–84.
[7] Post JW, Bhattacharyya A, Imran M. Experimental results and a user-friendly model of heat transfer from a thin film resistance temperature detector. AppliedThermalEngineering (2009);29:116–130.
[8] Arrazola PJ, Arriola I, Davies MA, Cooke AL, Dutterer BS. The effect of machinability on thermal fields in orthogonal cutting of AISI 4140 steel. CIRPAnnalsManufacturingTechnology (2008);57:65–68.
[9] Davies MA, Yoon H, Schmitz TL, Burns TJ, Kennedy MD. Calibrated thermal microscopy of the tool–chip interface in machining. Machiningscience technology (2003);7:167–190.
[10] Dewes R., Ng E, Chua K., Newton P., Aspinwall D. Temperature measurement when high speed machining hardened mould/die steel. Journal Materials Processing Technology 1999;92-93:293–301.
[11] Kline W, DeVor R, Lindberg J. The prediction of cutting forces in end milling with application to cornering cuts. InternationalJournal Machine Tool DesignResearch (1982);22:7–22.
[12] Jayaram S, Kapoor S, DeVor R. Estimation of the specific cutting pressures for mechanistic cutting force models. InternationalJournal Machine ToolsManufacture (2001);41:265–281.
[13] Budak E, Altintas Y, Armarego E. Prediction of milling force coefficients from orthogonal cutting data. Journal Manufacturing ScienceEngineering (1996);118:216–224.
[14] Song G, Sui S, Tang L. Precision prediction of cutting force in oblique cutting operation. TheInternationalJournal Advanced Manufacturing Technology (2015);81:553–562.
[15] Dinc C, Lazoglu I, Serpenguzel A. Analysis of thermal fields in orthogonal machining with infrared imaging. Journal Materials Processing Technology (2008);198:147–154.
[16] Müller B, Renz U. Time resolved temperature measurements in manufacturing. Measurement (2003);34:363–370.
[17] Arrazola PJ, Aristimuno P, Soler D, Childs T. Metal cutting experiments and modelling for improved determination of chip/tool contact temperature by infrared thermography. CIRPAnnalsManufacturingTechnology (2015);64:57–60.
[18] Nomura T, Moriguchi H, Tsuda K, Isobe K, Ikegaya A, Moriyama K. Material design method for the functionally graded cemented carbide tool. InternationalJournal Refractory MetalsHardMaterials 1999;17:397–404.
[19] Herve P, Cedelle J, Negreanu I. Infrared technique for simultaneous determination of temperature and emissivity. IP&T 2012;55:1–10.
[20] Soler D, Aristimuño PX, de-Buruaga MS, Garay A, Arrazola PJ. New Calibration method to measure Rake Face Temperature of the tool during Dry Orthogonal Cutting using Thermography. AppliedThermalEngineering (2018);137:74–82..
[21] Shi D, Liu Q, Zhu Z, Sun J, Wang B. Experimental study of the relationships between the spectral emissivity of brass and the temperature in the oxidizing environment. InfraredPhysics&Technology (2014);64:119–124.
[22] Karnati S. Thermographic investigation of laser metal deposition. Missouri University of Science and Technology, (2015).
[23] Saunders P. Radiation Thermometry: Fundamentals and Applications in the Petrochemical Industry. vol. TT78. SPIE Press; (2007).